

AD-A049 528

MISSISSIPPI STATE UNIV MISSISSIPPI STATE DEPT OF MECH--ETC F/G 11/4
MIXED-MODE FRACTURE OF GRAPHITE/EPOXY COMPOSITES.(U)
NOV 77 D H MORRIS

AFOSR-76-3058

UNCLASSIFIED

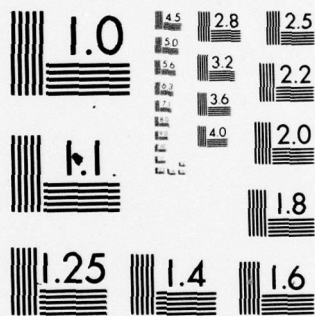
AFOSR-TR-78-0031

NL

191

ADAO49 528





MICROCOPY RESOLUTION TEST CHART
NATIONAL BUREAU OF STANDARDS-1963-A

AD A049528

AFOSR-TR- 78 - 0031

g (2)

MIXED-MODE FRACTURE
OF GRAPHITE/EPOXY COMPOSITES

by

Don H. Morris

November, 1977

FINAL TECHNICAL REPORT

Prepared under Grant No. AFOSR 76-3058

by

Mississippi State University
Department of Mechanical Engineering
Mississippi State, MS 39762

for

Air Force Office of Scientific Research
Bolling AFB
Washington, D.C. 20332

*See 1477
in
book*

DISTRIBUTION STATEMENT A

Approved for public release;
Distribution Unlimited

07 D D C
RECEIVED
FEB 2 1978
B

AD No. —
JDC FILE COPY

| REPORT DOCUMENTATION PAGE | | READ INSTRUCTIONS BEFORE COMPLETING FORM | |
|---|--|--|--|
| 1. REPORT NUMBER AFOSR-78-0031 | 2. GOVT ACCESSION NO. | 3. RECIPIENT'S CATALOG NUMBER | |
| 4. TITLE (and Subtitle) MIXED-MODE FRACTURE OF GRAPHITE/EPOXY COMPOSITES. | 5. TYPE OF REPORT & PERIOD COVERED FINAL rept. 1 June 76 - 1 Sep 77 | 6. PERFORMING ORG. REPORT NUMBER | |
| 7. AUTHOR(s) DON H. MORRIS | 8. CONTRACT OR GRANT NUMBER(s) AFOSR-76-3058 | 9. PROGRAM ELEMENT, PROJECT, TASK AREA & WORK UNIT NUMBERS 16 2307 17 B1 61102F | |
| 10. PERFORMING ORGANIZATION NAME AND ADDRESS MISSISSIPPI STATE UNIVERSITY MECHANICAL ENGINEERING DEPARTMENT MISSISSIPPI STATE, MS 39762 | 11. CONTROLLING OFFICE NAME AND ADDRESS AIR FORCE OFFICE OF SCIENTIFIC RESEARCH/NA BLDG 410 BOLLING AIR FORCE BASE, DC 20332 | 12. REPORT DATE Nov 77 | |
| 13. MONITORING AGENCY NAME & ADDRESS (if different from Controlling Office) | 14. NUMBER OF PAGES 31 | 15. SECURITY CLASS. (of this report) UNCLASSIFIED | |
| 16. DISTRIBUTION STATEMENT (of this Report) Approved for public release; distribution unlimited. | | 17. DISTRIBUTION STATEMENT (of the abstract entered in Block 20, if different from Report) | |
| 18. SUPPLEMENTARY NOTES | | | |
| 19. KEY WORDS (Continue on reverse side if necessary and identify by block number) COMPOSITES FRACTURE MIXED-MODE FRACTURE | | | |
| 20. ABSTRACT (Continue on reverse side if necessary and identify by block number) The reported research presents results on the fracture strength of graphite/epoxy (T300/5208) [0/+45] and [0/+45/90] symmetric laminates in the presence of angle cracks. The results indicate that the fracture strength can be predicted irrespective of the crack orientation if one uses the effective normal crack length in the equation developed for normal cracks. The fracture strength prediction is made using a two parameter (unnotched fracture strength and inferred dimensions of the damage zone) model, when the laminate is subjected to uniaxial loading along one of the material symmetry axes. The results indicate that the critical damage zone is not constant for the two laminates although it is independent of the crack orientation. | | | |

DD FORM 1 JAN 73 1473

EDITION OF 1 NOV 65 IS OBSOLETE

SECURITY CLASSIFICATION OF THIS PAGE (When Data Entered)

UNCLASSIFIED

391 810

JOB

ABSTRACT

The reported research presents results on the fracture strength of graphite/epoxy (T300/5208) $[0/\pm 45]$ and $[0/\pm 45/90]$ symmetric laminates in the presence of angle cracks. The results indicate that the fracture strength can be predicted irrespective of the crack orientation if one uses the effective normal crack length in the equation developed for normal cracks. The fracture strength prediction is made using a two parameter (unnotched fracture strength and inferred dimension of the damage zone) model, when the laminate is subjected to uniaxial loading along one of the material symmetry axes. The results indicate that the critical damage zone is not constant for the two laminates although it is independent of the crack orientation.

| | |
|---------------------------------|---|
| ACCESSION for | |
| NTIS | White Section <input checked="" type="checkbox"/> |
| DDC | Buff Section <input type="checkbox"/> |
| UNANNOUNCED | <input type="checkbox"/> |
| JUSTIFICATION _____ | |
| BY _____ | |
| DISTRIBUTION/AVAILABILITY CODES | |
| Dist. | AVAIL. and/or SPECIAL |
| A | |

AIR FORCE OFFICE OF SCIENTIFIC RESEARCH (AFSC)
NOTICE OF TRANSMITTAL TO DDC

This technical report has been reviewed and is
approved for public release IAW AIR 100-12 (7b).
Distribution is unlimited.

A. D. BLOSE
Technical Information Officer

TABLE OF CONTENTS

| | Page |
|--------------------------------|------|
| LIST OF TABLES | iv |
| LIST OF FIGURES | v |
| INTRODUCTION | 1 |
| EXPERIMENTAL PROGRAM | 2 |
| RESULTS | 3 |
| CONCLUSIONS | 7 |
| ACKNOWLEDGEMENTS | 8 |
| REFERENCES | 9 |
| TABLES | 11 |
| FIGURES | 15 |

LIST OF TABLES

| | Page |
|---|------|
| Table 1. Fracture Strengths | 11 |
| Table 2. Ultimate Strengths | 13 |
| Table 3. Critical Damage Zone Sizes | 14 |

LIST OF FIGURES

| | Page |
|---|------|
| Figure 1. Center-cracked tensile specimen. | 15 |
| Figure 2. Least squares fit for c_0 , angle crack, $[0/\pm 45/90]_s$ laminate. | 16 |
| Figure 3. Least squares fit for c_0 , normal crack, $[0/90/\pm 45]_s$ laminate. | 17 |
| Figure 4. Analytical model comparison for angle crack and normal crack. | 18 |
| Figure 5. Damage zone dimension vs. equivalent normal crack for $[0/\pm 45/90]_s$ laminate. | 19 |
| Figure 6. Damage zone dimension vs. initial crack for $[0/90/\pm 45]_s$ laminate. | 20 |
| Figure 7. Least squares fit for c_0 , angle crack, $[0/\pm 45]_s$ laminate. | 21 |
| Figure 8. Least squares fit for c_0 , normal crack, $[0/\pm 45]_s$ and $[0/\pm 45]_{2s}$ laminates. | 22 |
| Figure 9. Analytical model comparison for angle crack and normal crack. | 23 |
| Figure 10. Damage zone dimension vs. equivalent normal crack for $[0/\pm 45]_s$ laminate. | 24 |
| Figure 11. Effect of crack length and thickness on c_0 for $[0/\pm 45]$ laminate, normal crack. | 25 |
| Figure 12. Comparison of analytical and experimental results, T300/5208. | 26 |

INTRODUCTION

A review of the literature indicates that most of the work in fracture of composites has emphasized Mode I loading. By comparison, mixed-mode fracture has received little attention. Most of the available mixed-mode data falls in the category of unidirectional composites, with the crack being parallel to the fibers. For this case it has been observed that cracks oriented parallel to the fibers propagate along the fiber direction [1]. In addition, Wu [1] showed that the critical stress intensity factors K_{IC} and K_{IIc} are practically independent of crack length for fiber glass reinforced Scotchply.

For co-linear crack propagation a constant maximum energy release rate was suggested [1] as a possible fracture criterion. However, the data for Scotchply indicates that this criterion is not realistic.

McKinney [2], using unidirectional graphite/epoxy laminates with implanted cracks parallel to fibers, also found that the energy criterion was not applicable. Sanford and Stonesifer [3] reported contradicting results for glass reinforced plastics which seemed to show the validity of the energy criterion although the data does not include a measurement of K_{IIc} .

All of the mixed-mode fracture data previously cited was generated for unidirectional composites with crack parallel to the fiber direction. By comparison, less is known about composites where the layup is more general than the unidirectional. Brinson and Yeow [4] studied fracture of graphite/epoxy laminates using specimens cut at various angles to the principal material direction. Their results indicate that, in general, net fracture stresses tend to increase when the crack is aligned more closely

with the load direction. No attempt was made to analytically model the fracture behavior of single and double edge notched specimens.

Some of the available criteria for mixed-mode fracture of isotropic materials were discussed by Nuismer and Hahn [5]. On the whole, all the criteria except the one based on the energy release rate assume that the final fracture becomes imminent when failure occurs at a point some distance away from the crack tip. The failure functions considered include the circumferential stress [6], the principal stress, the Tresca-Guest and Huber-Mises-Hencky yield functions and a modified version [7], and the strain energy density [8]. Recently, Wu [9, 10] proposed the use of the polynomial failure criterion to predict fracture of glass/epoxy laminates.

In the present work, however, no attempt will be made to apply any of the aforementioned methods to the fracture of graphite/epoxy laminates. Rather, results are presented on the variation of the notched strength with the crack orientation angle relative to the load axis. A simple model based on the idea of an effective normal crack will be chosen to fit the data. This model can be useful in assessing the severity of ballistic impact damage in composite laminates.

EXPERIMENTAL PROGRAM

The experimental program consisted of determining the unnotched and notched fracture strengths of two composite laminate systems. It will be shown that a two parameter model can be used to predict the fracture strength of the laminates when subjected to uniaxial loading along one of the material symmetry axes.

The material used in the experimental program consisted of Thorne 300 graphite fibers in a Narmco 5208 epoxy resin. All test specimens

(see Figure 1) were 2-in. wide and 12-in. long (9-in. between end tabs). Cracks were produced by first drilling a small hole in a specimen followed by a final lengthening with a 5 mil diamond wire. No attempt was made to further sharpen the crack tips. Two crack lengths were used, 0.5-in. and 0.8-in. The angle θ (Figure 1) varied from 15° to 90° , in 15° increments.

The laminate orientations and number of test specimens may be summarized as:

$[0/\pm 45/90]_S$; three specimens for each crack length and angle

$[0/\pm 45]_S$; three specimens for each crack length and angle

Thus, a total of 72 specimens were tested to determine fracture loads as a function of laminate orientation, crack length, and angle of crack. The results are given in Table 1. In addition, four specimens of each laminate orientation were tested to determine the unnotched tensile strength; the results may be found in Table 2. The fiber volume fraction for each laminate was approximately 0.64.

All specimens, both notched and unnotched, were loaded by friction grips and tested in a closed-loop hydraulic machine at a constant load rate of 20 lb/sec. The environmental conditions were approximately constant at 70°F and 50% relative humidity.

RESULTS

Several models have been proposed in the literature for the prediction of the fracture strength of composite materials. Two models that are of interest in regard to the data herein are the inherent flaw model [11] and the average stress model [12, 13]. Both models have been used to predict the fracture strength of uniaxially loaded composites containing holes and cracks. In the case of cracks the average stress model [12, 13] becomes identical with the inherent flaw model of [11], as discussed in [14].

According to the above models, the ratio of the notched fracture strength to the unnotched tensile strength is given by

$$\frac{\sigma_{n\infty}}{\sigma_0} = \left(\frac{c_0}{a_0 + c_0} \right)^{1/2} \quad (1)$$

where: $\sigma_{n\infty}$ = notched fracture strength for an infinite plate
 σ_0 = unnotched tensile strength
 a_0 = original crack half-length
 c_0 = dimension of the damage zone at crack tips

The model given by Egn. (1) has been applied to composite laminates with center cracks perpendicular to the load axis. It will be shown that the same model can be applied to the angle crack problem, where the angle crack is treated as an equivalent normal crack having a length equal to the projection of the angle crack normal to the load axis. In other words, the original crack half-length, a_0 , is replaced by the equivalent normal crack half-length of magnitude $a_0 \sin \theta$, where θ is the angle between load axis and crack (Fig. 1). The damage zone dimension, c_0 , then retains the same meaning as for a normal crack.

The infinite plate notched fracture strength is calculated from the equation

$$\sigma_{n\infty} = Y \sigma_n \quad (2)$$

where: Y = finite width correction factor based on equivalent normal crack

σ_n = notched fracture strength of finite width specimen, based on gross cross sectional area

The value of Y is determined from the equation for isotropic materials [15],

$$Y = 1 + 0.128 (a/w) - 0.288 (a/w)^2 + 1.525 (a/w)^3 \quad (3)$$

where, for the angle crack problem, $2a$ is the equivalent normal crack ($2a_0 \sin \theta$) and $2w$ is the specimen width. The finite width correction factor for the $[0/\pm 45]_s$ laminate is slightly different from the isotropic value. However, the difference is less than 2% in the range of crack sizes considered [16].

The value of the damage zone, c_0 , is found empirically. Rewriting Eqn. (1) in the form

$$a_0 \sin \theta = \left[\left(\frac{\sigma_0}{\sigma_{n\infty}} \right)^2 - 1 \right] c_0 \quad (4)$$

results in an equation of a straight line, with c_0 as the slope. Note that Eqn. (4) has been written for the angle crack.

Figure 2 shows the results of the $[0/\pm 45/90]_s$ laminate with angle cracks. Three specimens of each crack length and angle were tested. Using a least squares fit the value of c_0 was found to be 0.113 in. (2.87 mm).

It is of interest to compare the value of c_0 found using angle cracks with that found using only normal cracks, for the same material system. The normal crack results are shown in Fig. 3, for the data of Ref. [17]. The values of c_0 for angle and normal cracks are within 6% from the average value.

Figure 4 compares the model prediction, Eqn. (1), for both the angle crack and normal crack. Note the insignificant difference in results regardless of the type of crack. Also, one additional comment is in order. The data for the normal crack is for a $[0/90/\pm 45]_s$ laminate [17]. However, the data of Whitney and Kim [18] indicates that the notched strength of quasi-isotropic graphite/epoxy laminates appears to be independent of

stacking sequence. Thus, for the stacking sequence indicated in Fig. 4, use of either the normal or angle crack results in essentially the same value of predicted notched strength. A comparison of Eqn. (1) with experimental results will be shown in a later figure.

To be of use, the value of c_0 in Eqn. (1) must remain constant for all crack sizes. Figures 5 and 6 show the effect of crack size on the damage zone dimension, for angle and normal cracks, respectively. The solid lines represent the least squares value of c_0 . A constant value of c_0 for different size cracks appears adequate.

Corresponding results for $[0/\pm 45]$ laminates may be seen in Figs. 7-11. All normal crack data was taken from Ref. [17]. Figure 7 shows data for angle cracks, whereas Fig. 8 combined data for two laminate thicknesses. The effect of thickness within the framework of the classical laminated plate theory is illustrated in Fig. 11, which shows different values of c_0 for the two laminates. Since smaller values of c_0 means higher notch sensitivity, i.e., more reduction in notched strength, the $[0/\pm 45]_s$ laminate is seen to be slightly more sensitive to cracks than is the $[0/\pm 45]_{2s}$ laminate. However, the difference is practically negligible and the average value is used in the subsequent analyses.

Figure 9 compares best fit fracture strengths for angle and normal cracks. The normal crack curve is drawn using c_0 from Fig. 8. As before, it is seen that predicted results are essentially the same regardless of whether c_0 is found using angle crack data or normal crack data.

Figure 12 shows both experimental results and analytical predictions, Eqn. (1), for two different laminates with angle cracks. The results indicate that the analytical model adequately predicts the notched strength of

laminates under uniaxial loading conditions. Even though there is more scatter in data for the quasi-isotropic laminate, the analytical model gives results that are conservative on the average.

For the $[0/\pm 45]$ laminates the value of c_0 obtained using the least square fit method is less than the value of c_0 obtained using compliance matching [17]. Consequently, the compliance matching method resulted in strength prediction higher than the experimental data.

Table 3 summarizes the average values of c_0 for the laminate systems and crack types studied. The results of this table indicate that the critical damage zone size c_0 is not constant for different laminates although it is independent of the crack orientation. Thus, c_0 should be found for each laminate, as was done in the present study.

CONCLUSIONS

It has been shown that a two parameter (unnotched fracture strength and inferred dimension of the damage zone) model can be successfully used to predict the fracture strength of composite laminates subjected to uniaxial loading along one of the material symmetry axes. The model is applicable regardless of the orientation of the crack, or the laminate system (at least for those laminate systems that have been tested). For the material system, T300/5208, and laminates, $[0/\pm 45]_s$ and $[0/\pm 45]_{2s}$, the data are essentially independent of laminate thickness.

However, the value of the dimension of the damage zone is different for each laminate system. Table 3 gives a comparison of the values of c_0 for the laminate systems and crack types studied. The results of this table indicate that the damage zone c_0 is not constant for various laminates although it is independent of the crack orientation.

ACKNOWLEDGEMENTS

The financial support provided for this work by AFOSR Mini-Grant 76-3058 is gratefully acknowledged. Further, sincere appreciation is extended to Mr. William J. Walker of the Air Force Office of Scientific Research for his encouragement. The author would also like to thank R. Cornwell and R. Esterline of the University of Dayton Research Institute for the fabrication, preparation, and testing of specimens.

REFERENCES

1. E. M. Wu and R. C. Reuter, "Crack Extension in Fiberglass Reinforced Plastics", University of Illinois TAM Report 275, 1965.
2. J. M. McKinney, "Mixed-Mode Fracture of Unidirectional Graphite/Epoxy Composites", J. Composite Materials, Vol. 6 (1972), p. 164.
3. R. J. Sanford and F. R. Stonesifer, "Fracture Toughness Measurements in Unidirectional Glass Reinforced Plastics", J. Composite Materials, Vol. 5 (1971), p. 241.
4. H. F. Brinson and Y. T. Yeow, "An Investigation of the Failure and Fracture Behavior of Graphite/Epoxy Laminates", Virginia Polytechnic Institute and State University Report, VPI-E-75-23, September 1975.
5. R. J. Nuismer and H. T. Hahn, "Mixed-Mode Fracture of Fiber Reinforced Composite Laminates", presented at the ASTM Composite Reliability Symposium, Las Vegas, Nevada, April 1974.
6. F. Erdogan and G. C. Sih, "On the Crack Extension in Plates Under Plane Loading and Transverse Shear", Trans ASME, Journal of Basic Engineering, Vol. 85 (1963), p. 519.
7. G. H. Lindsey, "Some Observations on Fracture Under Combined Loading", ASTM STP 536, American Society for Testing and Materials, 1973, p. 22.
8. G. C. Sih, E. P. Chen, S. L. Huang, and E. J. McQuillen, "Material Characterization on the Fracture of Filament-Reinforced Composites", J. Composite Materials, Vol. 9 (1975), p. 167.
9. E. M. Wu, "Strength and Fracture of Composites", in Composite Materials, Vol. 5, L. J. Broutman, Ed., Academic Press, N. Y., 1974, p. 191.
10. E. M. Wu, "Exploratory Development on Basic Failure Behavior of Anisotropic Polymeric Material", AFML-TR-74-77, Air Force Materials Laboratory, April, 1974.
11. M. E. Waddoups, J. R. Eisenmann, and B. E. Kaminski, "Macroscopic Fracture Mechanics of Advanced Composite Materials", J. Composite Materials, Vol. 5 (1971), p. 446.
12. J. M. Whitney and R. J. Nuismer, "Stress Fracture Criteria for Laminated Composites Containing Stress Concentrations", J. Composite Materials, Vol. 8 (1974), p. 253.
13. R. J. Nuismer and J. M. Whitney, "Uniaxial Failure of Composite Laminates Containing Stress Concentrations", ASTM-STP 593, American Society for Testing and Materials, 1975, p. 117.

14. S. W. Tsai and H. T. Hahn, "Failure Analysis of Composite Materials", in Inelastic Behavior of Composite Materials, AMD-- Vol. 13, American Society of Mechanical Engineers, 1975, p. 73.
15. W. F. Brown and J. E. Srawley, Plane Strain Crack Toughness Testing of High Strength Metallic Materials, ASTM-STP 410, American Society for Testing and Materials, 1966.
16. T. A. Cruse and J. R. Osias, "Exploratory Development on Fracture Mechanics of Composite Materials", AFML-TR-74-111, Air Force Materials Laboratory, April 1974.
17. D. H. Morris and H. T. Hahn, "Fracture Resistance Characterization of Graphite/Epoxy Composites," ASTM-STP 617, American Society for Testing and Materials, 1977, p. 5.
18. J. M. Whitney and R. Y. Kim, "Effect of Stacking Sequence on the Notched Strength of Laminated Composites", ASTM-STP 617, American Society for Testing and Materials, 1977, p. 229.

Table 1. Fracture Strengths


| SPECIMEN | LAMINATE [0/±45/90] _s | 2W(in.) | t(in.) | 2a ₀ (in.) | θ(deg.) | σ _n (ksi) |
|----------|--|---------|--------|-----------------------|---------|----------------------|
| 5-B-11 |  | 1.9974 | 0.0441 | 0.4958 | 15 | 41.10 |
| 6-T-8 | | 2.0010 | 0.0445 | 0.4931 | ↓ | 46.60 |
| 6-B-10 | | 2.0011 | 0.0446 | 0.5023 | 30 | 51.26 |
| 4-T-3 | | 1.9974 | 0.0456 | 0.5056 | ↓ | 41.28 |
| 4-B-10 | | 1.9975 | 0.0445 | 0.5047 | ↓ | 39.38 |
| 6-B-5 | | 1.9998 | 0.0456 | 0.4945 | 45 | 41.89 |
| 4-B-8 | | 1.9987 | 0.0452 | 0.4974 | ↓ | 38.74 |
| 5-B-3 | | 2.0009 | 0.0431 | 0.4999 | ↓ | 37.40 |
| 6-T-6 | | 2.0016 | 0.0446 | 0.4952 | ↓ | 36.97 |
| 4-B-6 | | 1.9992 | 0.0439 | 0.5247 | 60 | 36.46 |
| 5-T-6 | | 1.9986 | 0.0434 | 0.5117 | ↓ | 29.74 |
| 6-T-1 | | 2.0000 | 0.0444 | 0.5033 | 75 | 33.22 |
| 4-T-9 | | 1.9983 | 0.0456 | 0.5152 | ↓ | 33.58 |
| 4-B-4 | | 1.9978 | 0.0441 | 0.4913 | ↓ | 38.30 |
| 6-T-10 | | 1.9990 | 0.0442 | 0.5086 | 90 | 31.46 |
| 4-T-11 | | 1.9979 | 0.0449 | 0.4767 | ↓ | 38.00 |
| 5-B-9 | | 1.9999 | 0.0438 | 0.5000 | ↓ | 30.08 |
| 6-B-1 | | 1.9994 | 0.0444 | 0.5019 | ↓ | 30.13 |
| 4-B-11 | | 1.9965 | 0.0440 | 0.7962 | 15 | 39.49 |
| 6-T-5 | | 2.0018 | 0.0442 | 0.7969 | ↓ | 40.12 |
| 6-B-11 | | 1.9992 | 0.0456 | 0.8128 | ↓ | 47.47 |
| 4-B-9 | | 1.9978 | 0.0452 | 0.8118 | 30 | 33.78 |
| 6-T-4 | | 1.9987 | 0.0436 | 0.8085 | ↓ | 35.27 |
| 6-B-6 | | 2.0003 | 0.0455 | 0.8104 | ↓ | 29.94 |
| 4-T-6 | | 1.9988 | 0.0456 | 0.8073 | 45 | 30.28 |
| 6-T-2 | | 2.0004 | 0.0445 | 0.8072 | ↓ | 30.55 |
| 6-B-8 | | 1.9982 | 0.0449 | 0.8052 | ↓ | 31.88 |
| 5-T-7 | | 1.9978 | 0.0433 | 0.8082 | 60 | 24.97 |
| 5-B-6 | | 2.0001 | 0.0431 | 0.8041 | ↓ | 25.50 |
| 6-T-3 | | 2.0000 | 0.0441 | 0.7959 | ↓ | 24.94 |
| 4-T-10 | | 1.9985 | 0.0450 | 0.8098 | 75 | 27.69 |
| 5-T-9 | | 1.9990 | 0.0438 | 0.8098 | ↓ | 22.56 |
| 5-B-8 | | 1.9995 | 0.0429 | 0.8114 | ↓ | 21.33 |
| 5-T-11 | | 1.9973 | 0.0430 | 0.8017 | 90 | 28.41 |
| 6-B-4 | | 1.9988 | 0.0435 | 0.8021 | ↓ | 24.44 |
| 6-T-11 | | 1.9991 | 0.0449 | 0.8044 | ↓ | 26.74 |

Table 1. (cont.)

| SPECIMEN | LAMINATE | 2W(in.) | t(in.) | 2a ₀ (in.) | θ(deg.) | σ _n (ksi) |
|----------|----------------------|---------|--------|-----------------------|---------|----------------------|
| 1-T-4 | [0/±45] _s | 1.9980 | 0.0343 | 0.4956 | 15 | 47.57 |
| 1-B-7 | | 1.9972 | 0.0347 | 0.4949 | ↓ | 45.82 |
| 2-B-2 | | 1.9972 | 0.0340 | 0.4923 | ↓ | 46.76 |
| 2-T-7 | | 1.9966 | 0.0337 | 0.5005 | 30 | 37.89 |
| 3-T-10 | | 1.9965 | 0.0342 | 0.5007 | ↓ | 37.49 |
| 3-B-3 | | 1.9998 | 0.0339 | 0.5056 | ↓ | 36.29 |
| 1-B-11 | | 1.9972 | 0.0340 | 0.5042 | 45 | 32.84 |
| 2-B-6 | | 1.9942 | 0.0335 | 0.5021 | ↓ | 30.24 |
| 3-T-8 | | 1.9974 | 0.0340 | 0.5075 | ↓ | 31.29 |
| 2-T-11 | | 1.9962 | 0.0332 | 0.5046 | 60 | 30.63 |
| 3-T-6 | | 1.9978 | 0.0337 | 0.4981 | ↓ | 29.56 |
| 3-B-7 | | 1.9978 | 0.0338 | 0.4998 | ↓ | 28.88 |
| 1-B-5 | | 1.9973 | 0.0340 | 0.5092 | 75 | 26.87 |
| 2-T-2 | | 1.9981 | 0.0346 | 0.4973 | ↓ | 26.27 |
| 2-B-9 | | 1.9976 | 0.0340 | 0.5080 | ↓ | 28.86 |
| 2-B-11 | | 1.9965 | 0.0341 | 0.4933 | 90 | 28.35 |
| 3-T-2 | | 1.9983 | 0.0341 | 0.5132 | ↓ | 29.06 |
| 3-B-11 | | 1.9956 | 0.0335 | 0.5078 | ↓ | 26.63 |
| 1-T-8 | | 1.9975 | 0.0343 | 0.7991 | 15 | 38.68 |
| 1-B-8 | | 1.9975 | 0.0344 | 0.8033 | ↓ | 38.20 |
| 2-T-5 | | 1.9975 | 0.0337 | 0.7991 | ↓ | 37.29 |
| 1-B-10 | | 1.9979 | 0.0340 | 0.8135 | 30 | 27.53 |
| 2-T-8 | | 1.9966 | 0.0345 | 0.7950 | ↓ | 27.00 |
| 2-B-5 | | 1.9952 | 0.0340 | 0.8049 | ↓ | 27.27 |
| 1-B-2 | | 1.9982 | 0.0344 | 0.7895 | 45 | 24.44 |
| 3-T-7 | | 1.9953 | 0.0331 | 0.8026 | ↓ | 25.51 |
| 3-B-6 | | 1.9978 | 0.0338 | 0.8014 | ↓ | 28.73 |
| 1-T-9 | | 1.9972 | 0.0358 | 0.7953 | 60 | 22.73 |
| 2-T-1 | | 1.9971 | 0.0335 | 0.7963 | ↓ | 26.38 |
| 3-T-5 | | 1.9971 | 0.0330 | 0.8095 | ↓ | 24.73 |
| 1-T-10 | | 1.9968 | 0.0338 | 0.8004 | 75 | 22.45 |
| 1-B-6 | | 1.9971 | 0.0338 | 0.8184 | ↓ | 20.44 |
| 2-B-10 | | 1.9969 | 0.0342 | 0.8108 | ↓ | 20.72 |
| 1-B-4 | | 1.9973 | 0.0340 | 0.8052 | 90 | 21.50 |
| 2-T-6 | | 1.9977 | 0.0341 | 0.8020 | ↓ | 19.67 |
| 3-B-10 | | 1.9966 | 0.0329 | 0.8145 | ↓ | 22.45 |

Table 2. Ultimate Strengths

| Laminate | Width (in) | Thickness (in) | Strength (ksi) |
|-------------------------|---------------|-------------------|-------------------|
| [0/±45] _s | 0.9462 | 0.0351 | 71.66 |
| | 0.9920 | 0.0351 | 70.65 |
| | 0.9477 | 0.0344 | 72.70 |
| | 0.9864 | 0.0335 | 64.46 |
| Average | 0.9681 | 0.0345 | 69.87 |
| C.V. (%) | 2.39 | 4.92 | 5.21 |
| [0/±45/90] _s | 0.9495 | 0.0453 | 58.12 |
| | 0.9908 | 0.0457 | 59.63 |
| | 0.9497 | 0.0427 | 55.51 |
| | 0.9908 | 0.0436 | 54.40 |
| Average | 0.9702 | 0.0443 | 56.91 |
| C.V. (%) | 2.45 | 5.03 | 4.47 |

Table 3. Critical Damage Zone Sizes

| Laminate | Type of Crack | c_0 , in. (mm) |
|-------------------|---------------|------------------|
| $[0/\pm 45]_s$ | Normal | 0.054 (1.372) |
| $[0/\pm 45]_{2s}$ | Normal | 0.054 (1.372) |
| $[0/90/\pm 45]_s$ | Normal | 0.100 (2.540) |
| $[0/\pm 45]_s$ | Angle | 0.049 (1.245) |
| $[0/\pm 45/90]_s$ | Angle | 0.113 (2.870) |

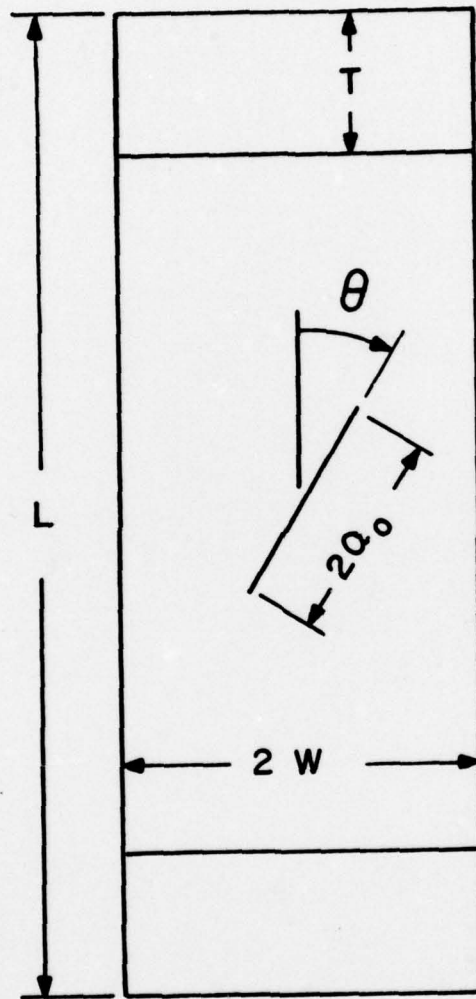


Figure 1. Center-cracked tensile specimen.

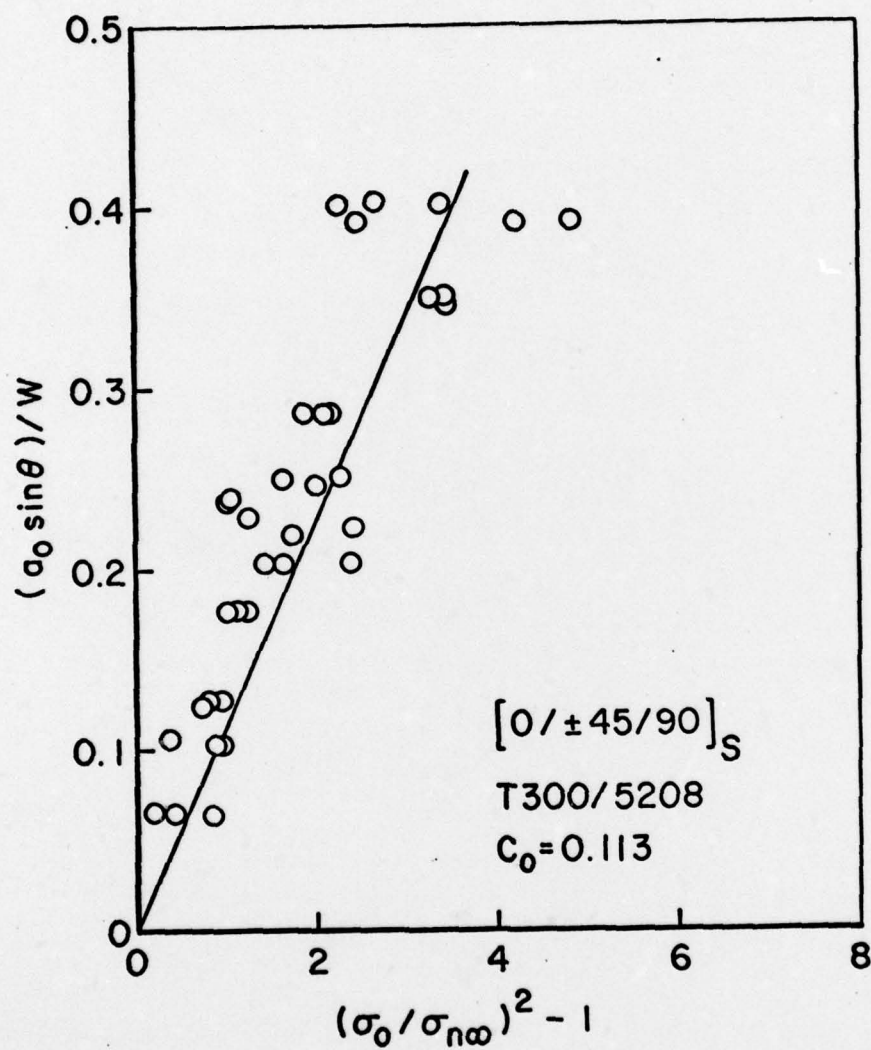


Figure 2. Least squares fit for c_0 , angle crack, $[0/\pm 45/90]_S$ laminate.

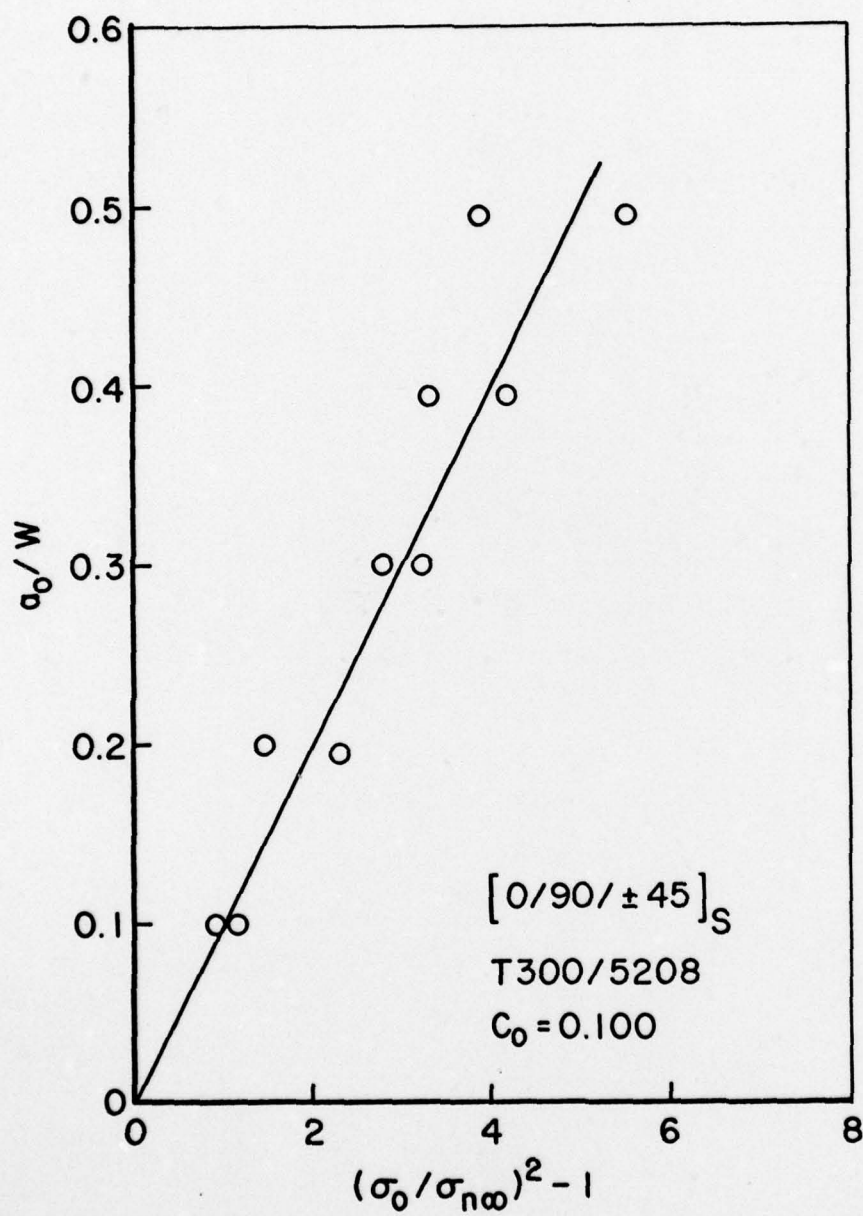


Figure 3. Least squares fit for c_0 , normal cracks, $[0/90/\pm 45]_S$ laminate.

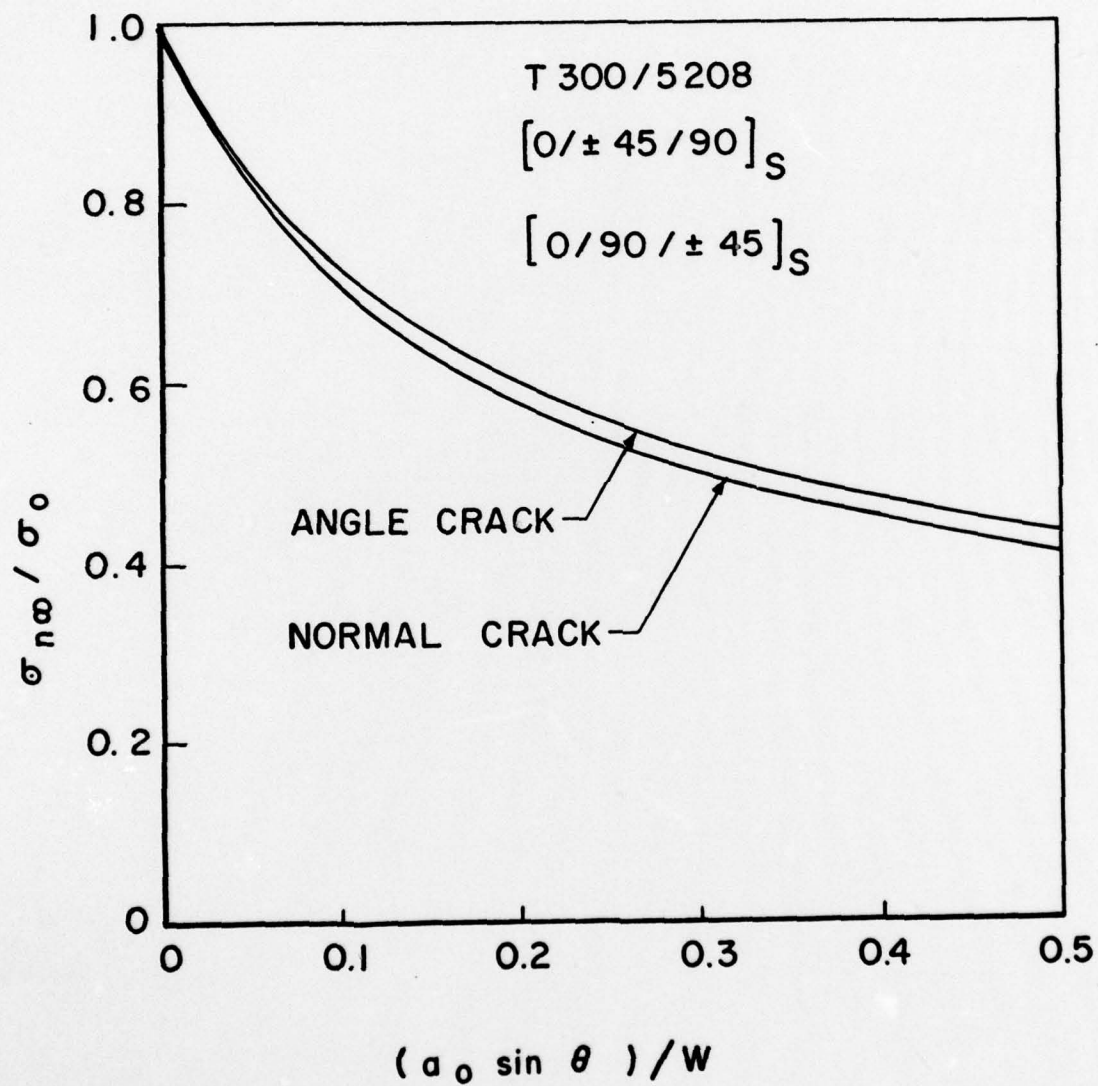


Figure 4. Analytical model comparison for angle crack and normal crack.

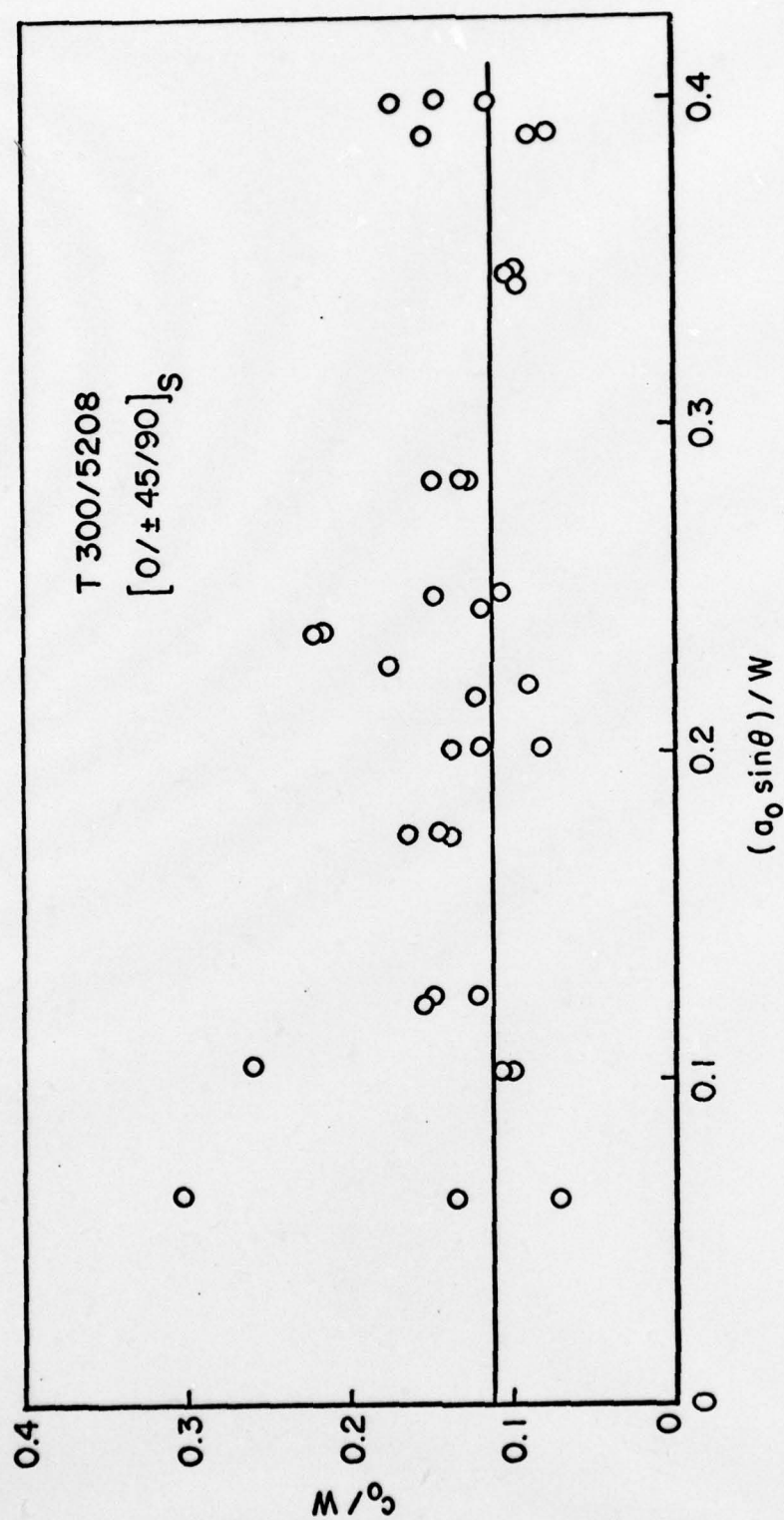


Figure 5. Damage zone dimension vs. equivalent normal crack for $[0/\pm 45/90]_S$ laminate.

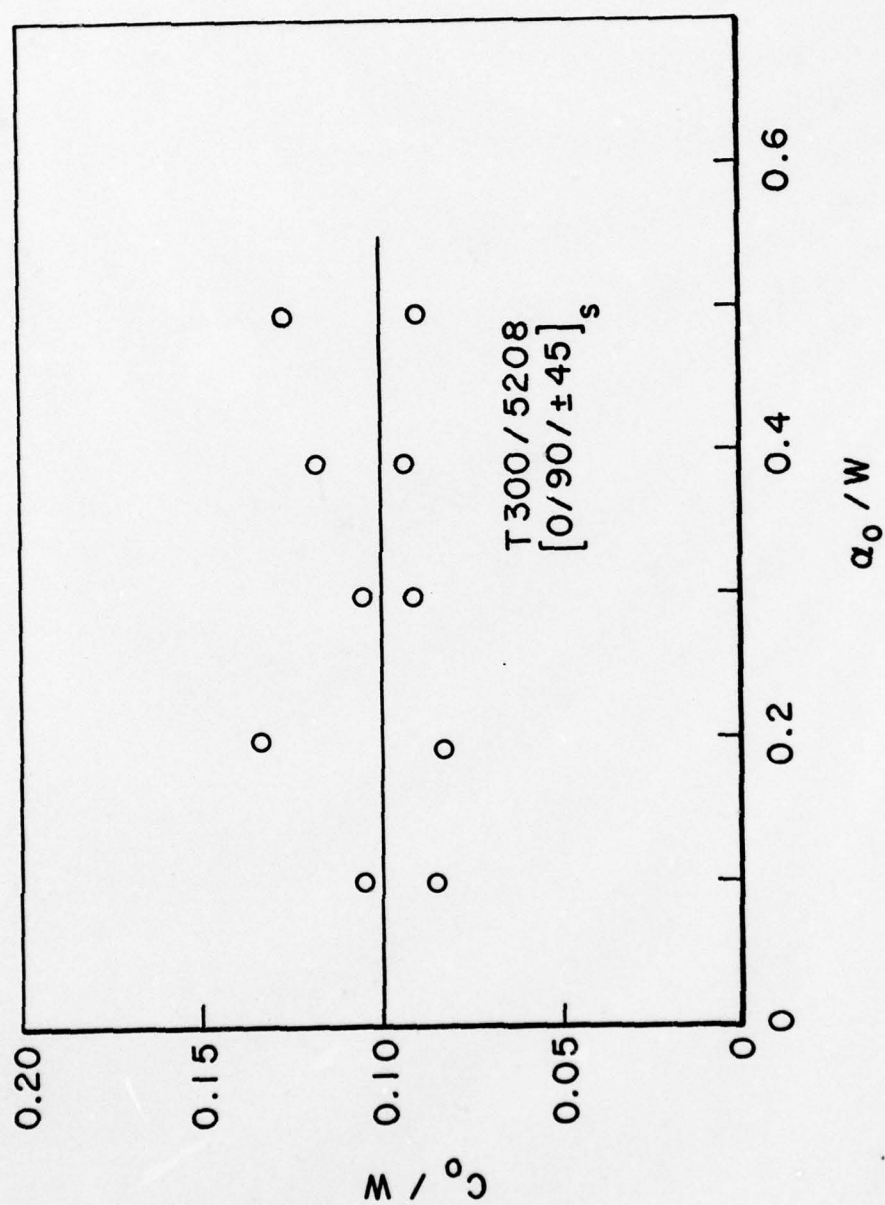


Figure 6. Damage zone dimension vs. initial crack for $[0/90/\pm 45]_s$ laminate.

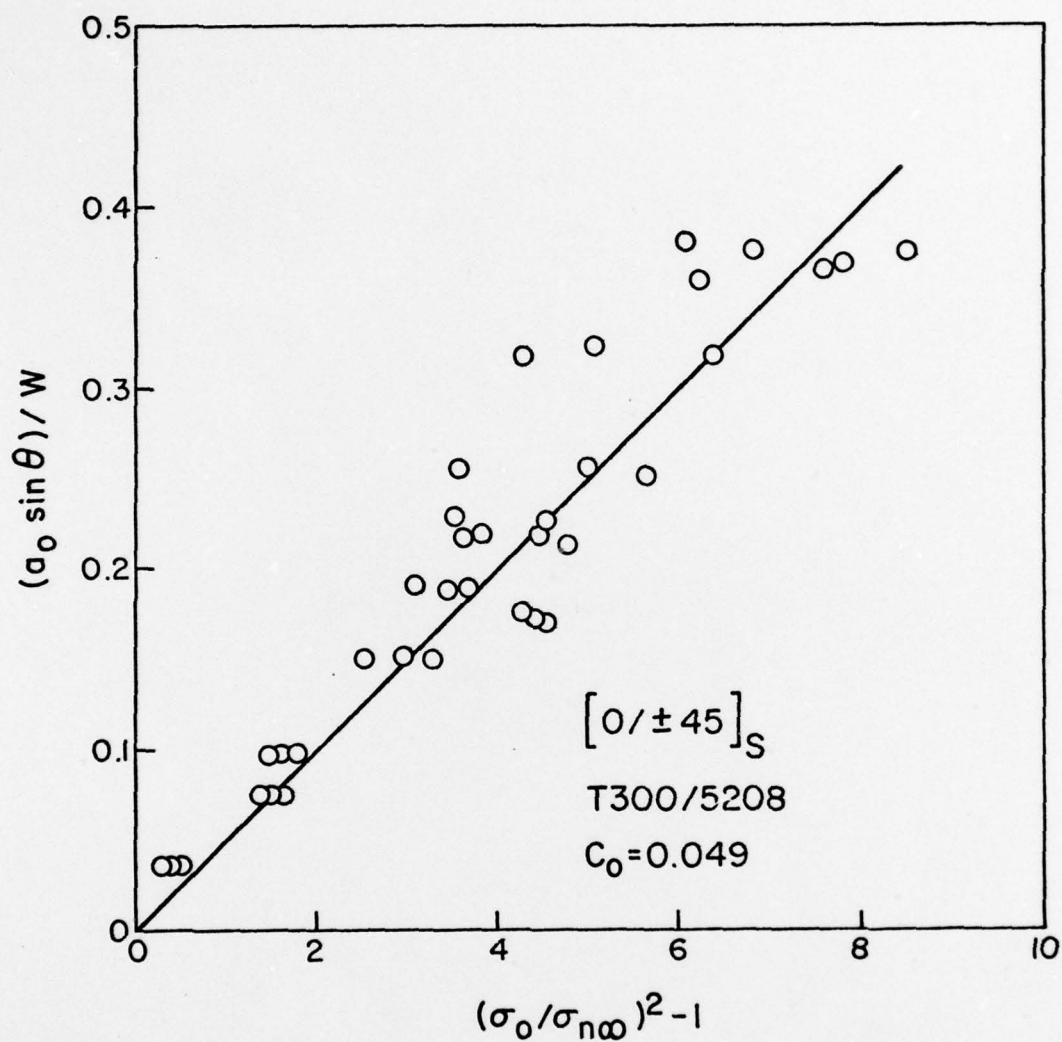


Figure 7. Least squares fit for c_0 , angle crack, $[0/\pm 45]_S$ laminate.

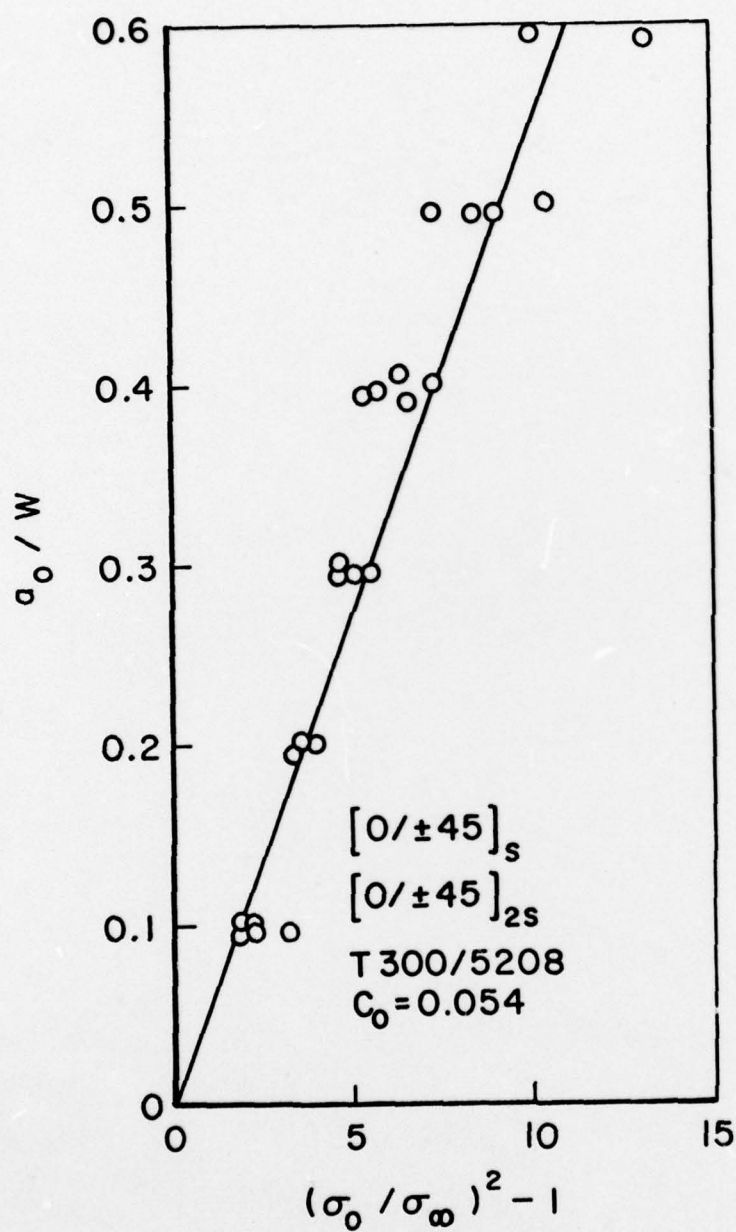


Figure 8. Least squares fit for c_0 , normal crack, $[0/\pm 45]_s$ and $[0/\pm 45]_{2s}$ laminates.

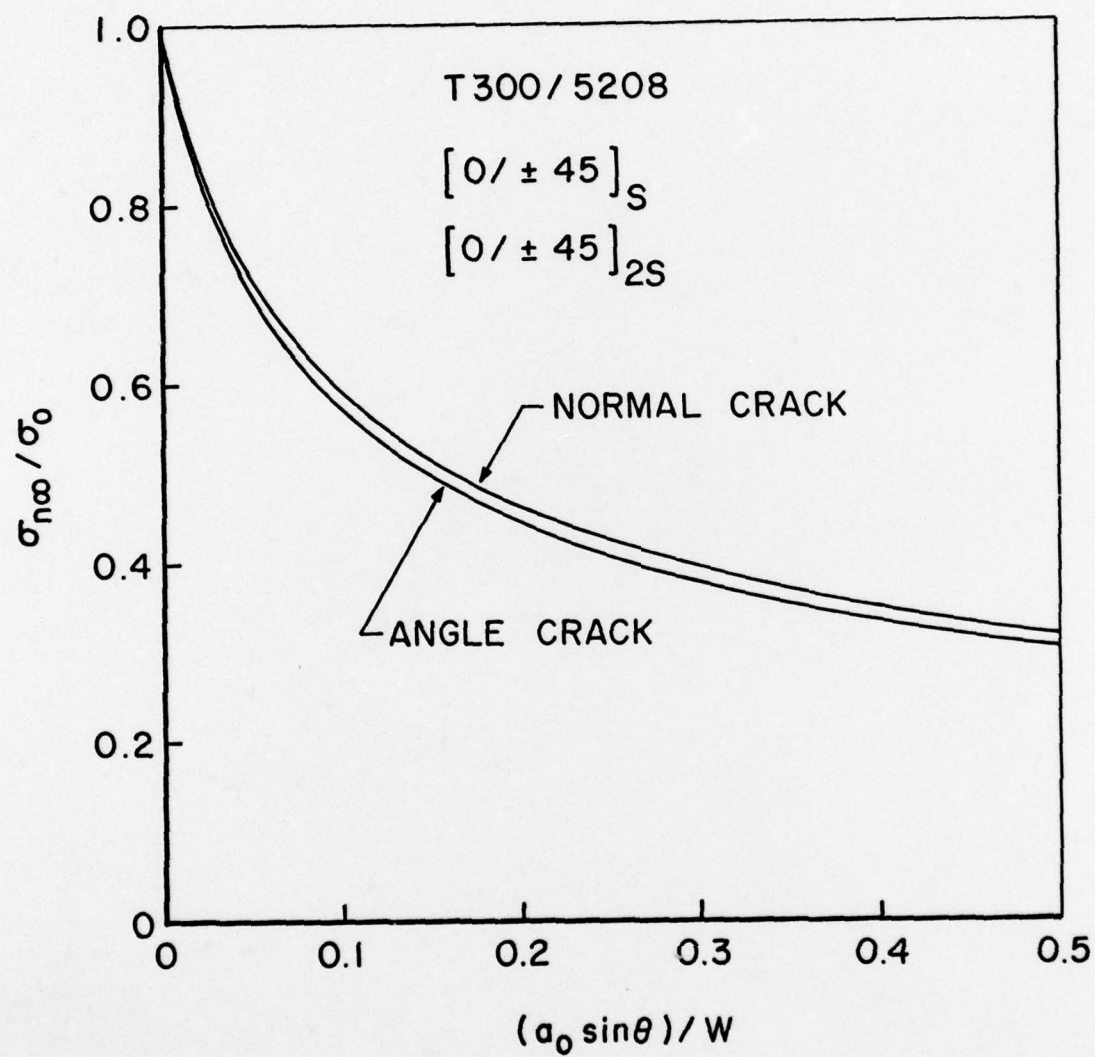


Figure 9. Analytical model comparison for angle crack and normal crack.

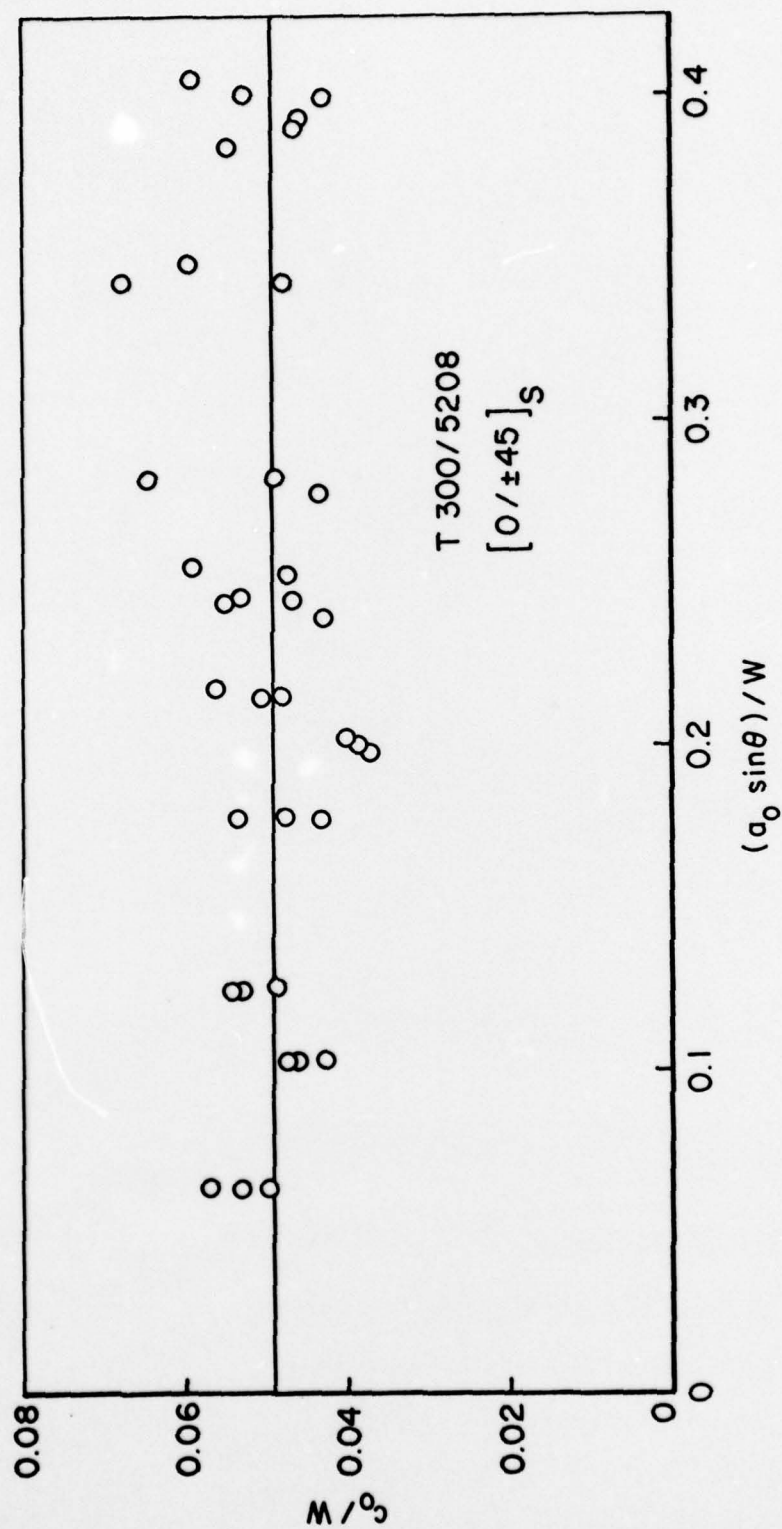


Figure 10. Damage zone dimension vs. equivalent normal crack for [0/±45]_S laminate.

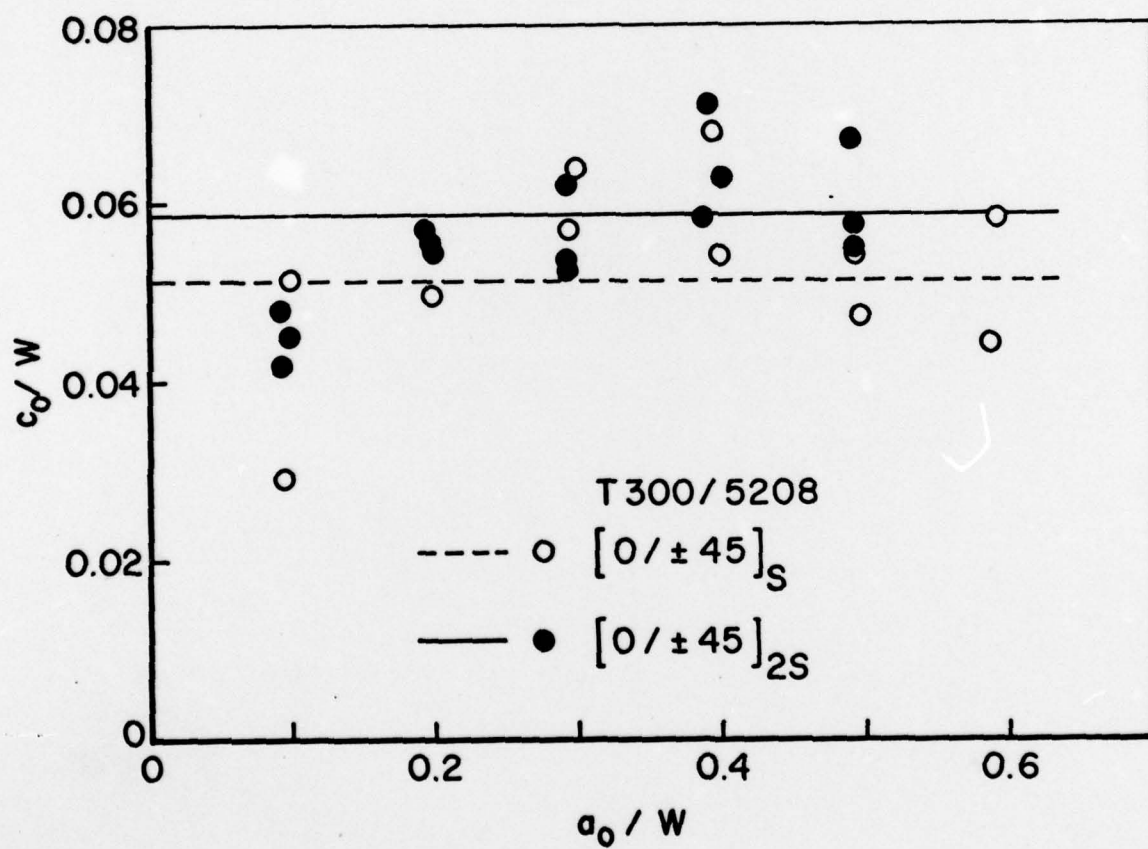


Figure 11. Effect of crack length and thickness on c_0 for $[0/\pm 45]$ laminate, normal crack.

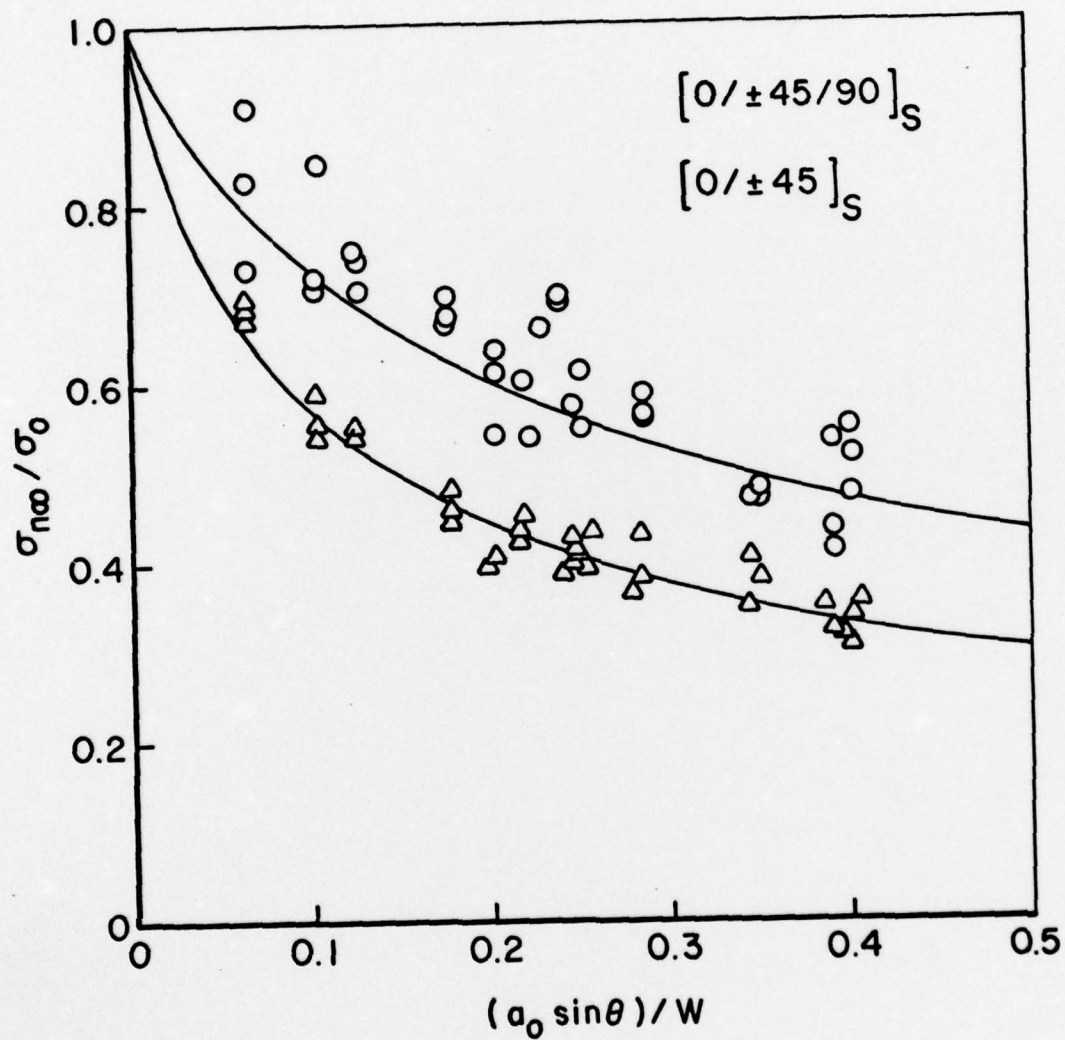


Figure 12. Comparison of analytical and experimental results, T300/5208.